Available online at www.sciencedirect.com
ScienceDirect
Journal of the European Ceramic Society 31 (2011) 2083–2087
www.elsevier.com/locate/jeurceramsoc

Spark plasma sintering of Al_2O_3–cBN composites facilitated by Ni nanoparticle precipitation on cBN powder by rotary chemical vapor deposition

Jianfeng Zhang, Rong Tu, Takashi Goto *

Institute for Materials Research, Tohoku University, Sendai 980-8577, Japan

Received 9 February 2011; received in revised form 1 May 2011; accepted 16 May 2011

Abstract

Al_2O_3–cBN/Ni composites were consolidated by spark plasma sintering (SPS) using α-Al_2O_3 and Ni nanoparticle precipitated cBN (cBN/Ni) powders. The Ni nanoparticles, 10–100 nm in diameter and 0.5–2.2 mass% in content, were precipitated on cBN powder by rotary chemical vapor deposition. The effect of sintering temperature (T_{SPS}) and Ni content (C_{Ni}) on the densification, phase transformation, microstructure and hardness of the Al_2O_3–cBN/Ni composites were investigated. The highest relative density of Al_2O_3–30 vol% cBN composite was 99% at T_{SPS} = 1573 K and C_{Ni} = 1.7 mass%. At T_{SPS} = 1673 K, the relative density decreased due to the phase transformation of cBN to hBN. The Vickers hardness of Al_2O_3–30 vol% cBN/Ni at T_{SPS} = 1573 K and C_{Ni} = 1.7 mass% showed the highest value of 27 GPa.

Keywords: Ni nanoparticle precipitated cBN (cBN/Ni); Spark plasma sintering (SPS); Phase transformation; Microstructure; C. Mechanical properties

1. Introduction

Cubic boron nitride (cBN) has been widely applied in cutting tools due to its being the hardest material after diamond,[1] its good thermal conductivity and its lesser reactivity with iron than diamond. However, cBN is hard to densify by conventional sintering because of the strong covalent bond and low self-diffusion coefficients of B and N.[2,3] Furthermore, the phase transformation of cBN to hexagonal BN (hBN) at high temperatures leads to a volume expansion resulting in cracking and low hardness. Therefore, monolithic cBN and cBN-based composites are compacted at an ultra-high pressure of more than several GPa.[4–6]

However, cBN-containing composites have been prepared by hot isostatic pressing (HIP) and spark plasma sintering (SPS) under moderate pressure. Martinez et al. sintered cBN–WC/Co composites with cBN contents up to 50 vol% at 1373–1473 K under pressures of 150 and 200 MPa by HIP.[7] The cBN–WC/Co composites showed a hardness of about 25 GPa, much higher than that of WC/Co. Since SPS can compact ceramics and composites at a relatively low temperature and short time,[8–11] the phase transformation of cBN to hBN can be depressed.[2,12] Hotta and Goto have prepared dense SiAlON–cBN[13] and Al_2O_3–cBN[14] composites containing 10–20 vol% cBN by SPS. The Vickers hardness of Al_2O_3–(10–20 vol%)cBN composites was 26 GPa, about 4 GPa higher than that of the monolithic Al_2O_3 body. The highest hardness of SiAlON–cBN was 16 GPa with 10 vol% cBN. In these composites, cBN was uniformly dispersed in Al_2O_3 and SiAlON matrices. However, with increasing cBN content higher than 30 vol%, the relative density of the composites decreased because the self-contact between cBN particles became significant. In order to prevent the self-contact of cBN particles, preliminary coating of additives directly on cBN particles may be promising.

Ni nanoparticle is a promising sintering additive as reported for Al_2O_3,[15–17] Al_2O_3–ZrO_2,[18] TiN–TiB_2[19] and WC.[20] However, no research has been published on Ni nanoparticle addition to sinter cBN –containing composites. In the present study, Ni nanoparticles were precipitated on cBN powder (hereafter cBN/Ni) by using RCVD (rotary chemical vapor deposition), and subsequently, Al_2O_3–cBN/Ni composites were consolidated by SPS. This paper reports the effect of Ni nanoparticle

* Corresponding author.
E-mail address: goto@imr.tohoku.ac.jp (T. Goto).

0955-2219/$ – see front matter © 2011 Elsevier Ltd. All rights reserved.
doi:10.1016/j.jeurceramsoc.2011.05.019

content on the relative density, Vickers micro-hardness, phase transformation and microstructures of the Al_2O_3–cBN/Ni composites.

2. Experimental details

Ni nanoparticles were precipitated on cBN powder (Showadenko, 2–4 μm in diameter) by RCVD using nickelocene ($NiCp_2$) as a precursor. $NiCp_2$ was evaporated at 393–423 K and carried into a reaction chamber by Ar at a flow rate of $1.67 \times 10^{-6}\ m^3\ s^{-1}$. The supply rate of $NiCp_2$ (R_s) was varied from 0.28 to 1.12 mg s^{-1}. Oxygen at a flow rate from 0.17 to $0.68 \times 10^{-6}\ m^3\ s^{-1}$ was introduced into the reaction chamber to eliminate carbon contamination. The reaction chamber was externally heated at 823 K and rotated at a rate of 45 rpm to keep the cBN powder continuously floating in the reaction chamber. The total pressure in the reaction chamber was maintained at 800 Pa. The deposition time was fixed at 1.8 ks.

CBN/Ni powder was mechanically mixed with α-Al_2O_3 powder and consolidated by spark plasma sintering (SPS-210LX, SPS Syntex Inc, Japan) with a graphite die (ϕ30 mm × ϕ10 mm × 30 mm) at a sintering temperature (T_{SPS}) of 1473–1673 K. A carbon sheet 0.2 mm in thickness was inserted between the raw material powder and the graphite die. The graphite die was wrapped with carbon blankets in order to minimize the heat loss in the sintering process. The heating rate in SPS was 1.67 K s^{-1} with a holding time of 0.6 ks under a uniaxial pressure of 100 MPa. The temperature was measured by an optical pyrometer in a hole (ϕ2 mm × 5 mm) on the die surface.

The crystal phase of the cBN/Ni powder and that of the Al_2O_3–cBN/Ni composites were identified by X-ray diffraction (XRD, Rigaku: RAD-2C, CuKα). The microstructure was observed by scanning electron microscopy (SEM, Hitach: S-3100H) and transmission electron microscopy (TEM, JEOL: 2000EX). The Ni content (C_{Ni}) in the cBN/Ni powder was estimated from energy-dispersive X-ray spectroscopy (EDS), and was averaged by five measurements in different areas. The density of the Al_2O_3–cBN/Ni composites was determined by an Archimedes' method and the relative density (D_r) was calculated from that of Al_2O_3 (3.99 g/cm^3),[21] cBN (3.49 g/cm^3)[22] and Ni (8.91 g/cm^3).[23] Vickers micro-hardness (H_v) at room temperature was measured by a hardness tester (HM-221, Mitsutoyo Corp.) at a load (P) of 0.98 N and was averaged by ten points.

3. Results and discussion

Fig. 1 shows the XRD patterns of cBN and cBN/Ni powders prepared at R_s = (a) 0.28, (b) 0.56, (c) 0.84 and (d) 1.12 mg s^{-1}. The oxygen flow rate (F_{O_2}) was (a) 0.17, (b) 0.34, (c) 0.51 and (d) $0.68 \times 10^{-6}\ m^3\ s^{-1}$, respectively. The diffraction peaks at $2\theta = 43.2°$ (1 1 1), 50.3° (2 0 0), and 74.1° (2 2 0) were indexed to Ni (Fig. 1(b)–(d)), and no NiO and C peaks were detected. The Ni intensity increased with increasing R_s, indicating that the Ni content increased. Fig. 2 shows the effect of R_s on C_{Ni} estimated from EDS. The C_{Ni} increased from 0.6 to 2.2 mass% with

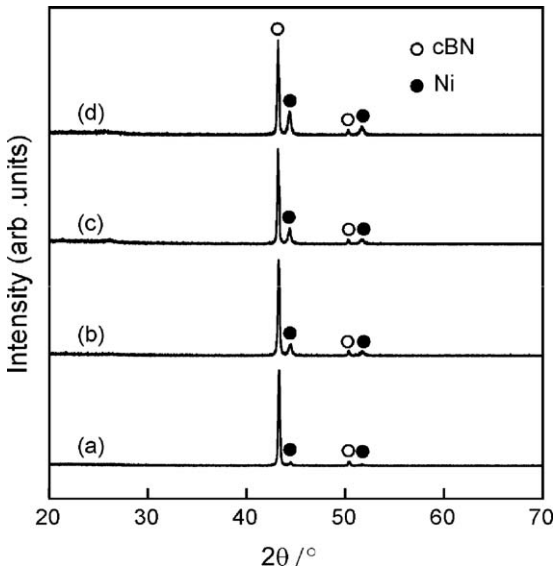

Fig. 1. X-ray diffraction (XRD) patterns of Ni-precipitated cBN powders at R_s = (a) 0.28, (b) 0.56, (c) 0.84 and (d) 1.12 mg s^{-1}.

increasing R_s from 0.28 to 1.12 mg s^{-1}. Fig. 3 shows the surface morphology of cBN/Ni powder at R_s = 0.28 to 1.12 mg s^{-1}. At R_s = 0.28 mg s^{-1}, Ni nanoparticles of about 10–20 nm in diamater were sparely distributed on the surface of cBN powder (Fig. 3(a)). At R_s = 0.56 mg s^{-1}, the amount of Ni nanoparticles increased apparently compared to that at R_s = 0.28 mg s^{-1} (Fig. 3(b)). At R_s = 0.84 to 1.12 mg s^{-1} (Fig. 3(c) and (d)), the Ni nanoparticles agglomerated to a diameter larger than 100 nm.

Fig. 4 shows the effect of C_{Ni} on the crystal phase of Al_2O_3–30 vol% cBN/Ni composite at T_{SPS} = 1573 K. At C_{Ni} = 0.6 and 1.2 mass%, α-Al_2O_3, cBN and Ni were identified (Fig. 4(a) and (b)). At C_{Ni} higher than 1.7 mass% (Fig. 4(c) and (d)), hBN was detected. Hotta and Goto have reported that the phase transformation from cBN to hBN was observed in Al_2O_3–cBN composites at T_{SPS} = 1673 K.[14] Thus, the phase transformation temperature of cBN to hBN in this work was

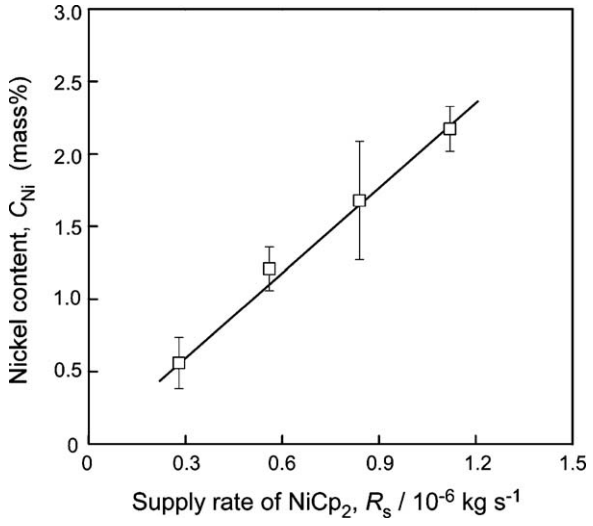

Fig. 2. Effect of R_s on the Ni content (C_{Ni}) in the Ni nanoparticle precipitated cBN.

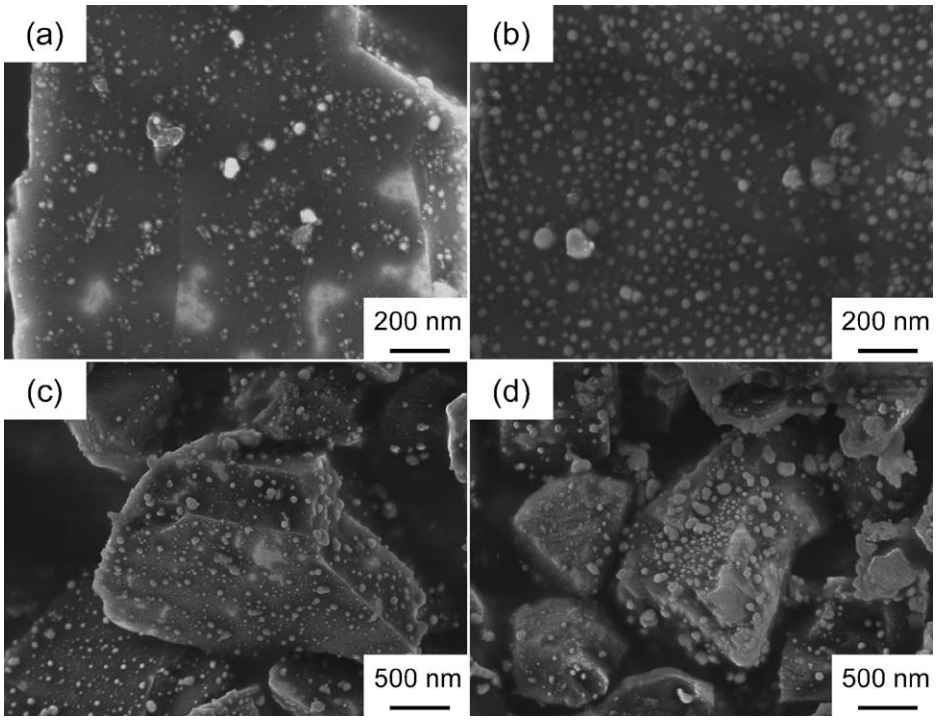

Fig. 3. FESEM images of Ni precipitated cBN powders at R_s = (a) 0.28, (b) 0.56, (c) 0.84 and (d) 1.12 mg s^{-1}.

about 100 K lower than that in Al_2O_3–cBN composites. This suggests that Ni nanoparticles may accelerate the phase transformation. On the other hand, it may also take place even at lower concentration, but the amount of transformation within the given time may be too small to be identified by XRD. Many researchers have reported that the incorporation of metal phases affect the thermal stability of cBN by accelerating reactions between metals and cBN,[5,24] and accelerating the transformation from cBN to hBN.[7] No reaction between cBN and Ni was identified in this work, while the phase transformation of cBN to hBN was promoted by catalytic activity of Ni nanoparticles.

Fig. 5 shows the effect of C_{Ni} on D_r of Al_2O_3–30 vol% cBN/Ni composite at T_{SPS} = 1473 to 1673 K. At T_{SPS} = 1473, the D_r of Al_2O_3–30 vol% cBN/Ni composite at C_{Ni} = 0.6 to 2.2 mass% was about 96%, almost independent of C_{Ni}. At T_{SPS} = 1573 K, the D_r of Al_2O_3–30 vol% cBN composite without Ni nanoparticles was 97%, slightly higher than that at T_{SPS} = 1473 K. At C_{Ni} = 0.6 to 1.7 mass%, the D_r of the Al_2O_3–30 vol% cBN/Ni composite was 99%. At C_{Ni} = 2.2 mass%, the D_r of the Al_2O_3–30 vol% cBN/Ni composite slightly decreased to 98.5%. At T_{SPS} = 1673 K, the D_r

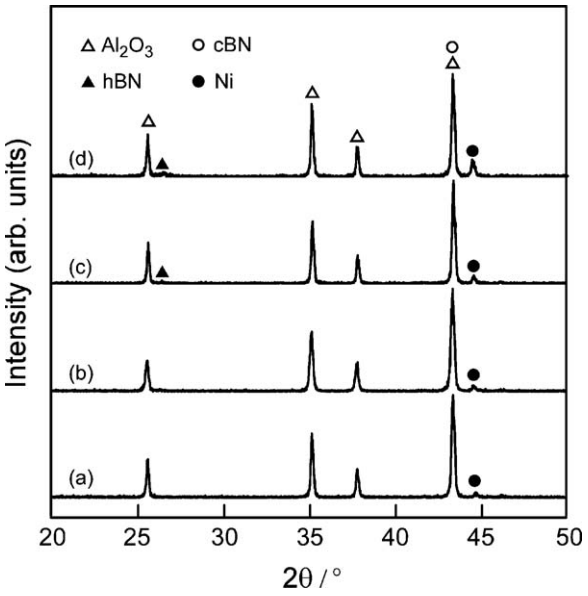

Fig. 4. XRD patterns of Al_2O_3–30 vol% cBN/Ni composite sintered at 1573 K with C_{Ni} = (a) 0.6, (b) 1.2, (c) 1.7 and (d) 2.2 mass%.

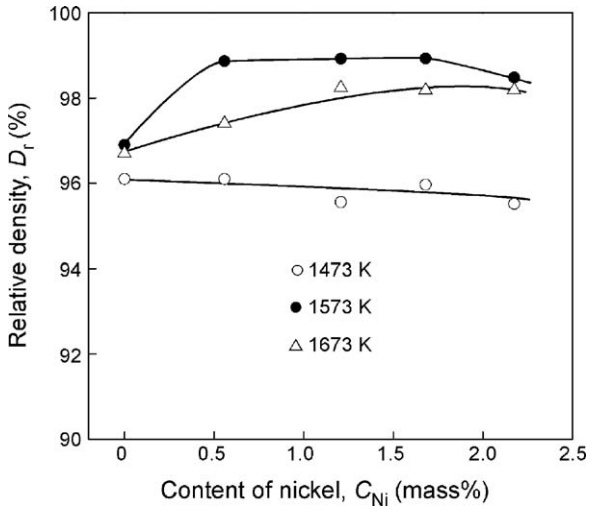

Fig. 5. Effect of Ni content on the relative density of Al_2O_3–30 vol% cBN/Ni composite sintered at 1473, 1573 and 1673 K for 600 s.

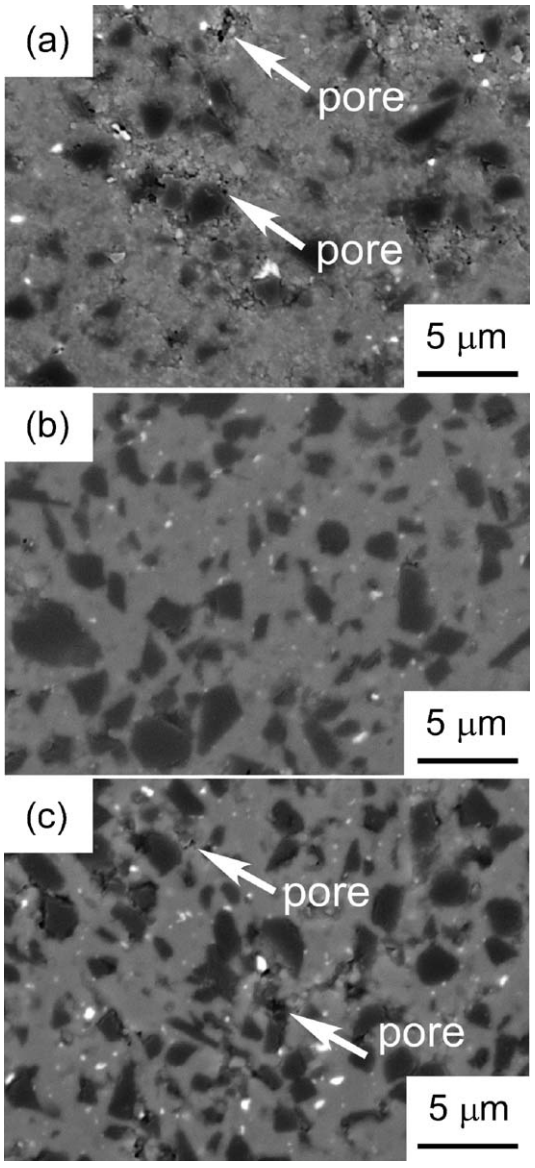

Fig. 6. SEM micrographs of the polished surface of Al_2O_3–30 vol% cBN/Ni composite sintered at (a) 1473, (b) 1573 and (c) 1673 K. (C_{Ni} = 1.7 mass%)s.

of Al_2O_3–30 vol% cBN/Ni composite increased from 96.7% to 98.2% with increasing C_{Ni} from 0 to 2.2 mass%, being lower than those at T_{SPS} = 1573 K due to the phase transformation of cBN to hBN.

Fig. 6 presents SEM images of the Al_2O_3–30 vol% cBN/Ni composite (C_{Ni} = 1.7 mass%) at T_{SPS} = 1473 to 1673 K. The arrows represent the presence of pores in the polished surfaces. EDS identified the black and white phases as being cBN and Ni, respectively. The Ni nanoparticles agglomearted into large grains from 0.1 to 1 μm in diameter. At T_{SPS} = 1473 K, some small pores existed due to a low relative density of the Al_2O_3–30 vol% cBN/Ni composite (arrows in Fig. 6(a)). At T_{SPS} = 1573 K, cBN particles were well bonded with Al_2O_3 matrix and no pores were observed (Fig. 6(b)). At T_{SPS} = 1673 K, pores were observed at the interface between Al_2O_3 and cBN grains (arrows in Fig. 6(c)). The pores could have caused by the volume change by the transformation of cBN to hBN.

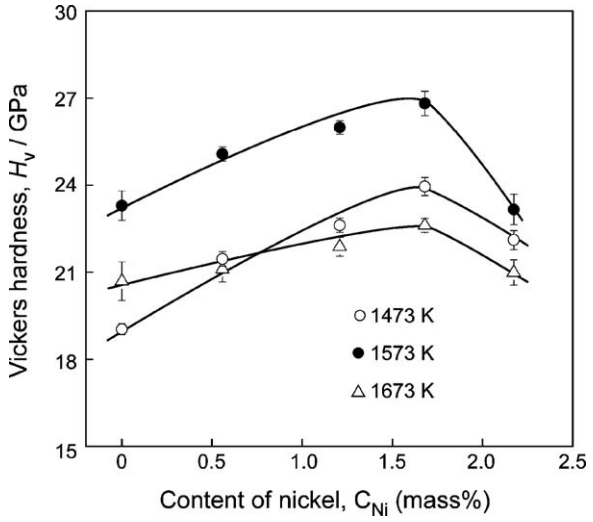

Fig. 7. Effect of Ni content on the Vickers hardness of Al_2O_3–30 vol% cBN/Ni composite sintered at 1473, 1573 and 1673 K for 600 s.

Fig. 7 shows the effect of C_{Ni} on the H_v of Al_2O_3–30 vol% cBN/Ni composite (C_{Ni} = 0–2.2 mass% at T_{SPS} = 1473 to 1673 K. The H_v of Al_2O_3–cBN/Ni composites showed the maximum at C_{Ni} = 1.7 mass%. The H_v at T_{SPS} = 1573 K was higher than those at T_{SPS} = 1473 and 1673 K. The highest H_v of the Al_2O_3–30 vol% cBN/Ni composite was 27 GPa at C_{Ni} = 1.7 mass% and T_{SPS} = 1573 K. Fig. 8 summarizes the effect of cBN content (C_{cBN}) on the H_v of the Al_2O_3–cBN/Ni composites. The Al_2O_3–cBN composites without Ni nanoparticles showed the maximum value of 26 GPa at C_{cBN} = 20 vol% and then significantly decreased at higher C_{cBN}. The Al_2O_3–cBN/Ni (C_{Ni} = 1.7 mass%) showed the maximum value of 27 GPa at C_{cBN} = 30 vol%. This value (27 GPa) was the highest value among cBN containing composites consolidated by the moderate pressure methods of SPS and HIP, i.e., Al_2O_3–cBN[14] (26 GPa), SiAlON–cBN (16 GPa),[13,25]

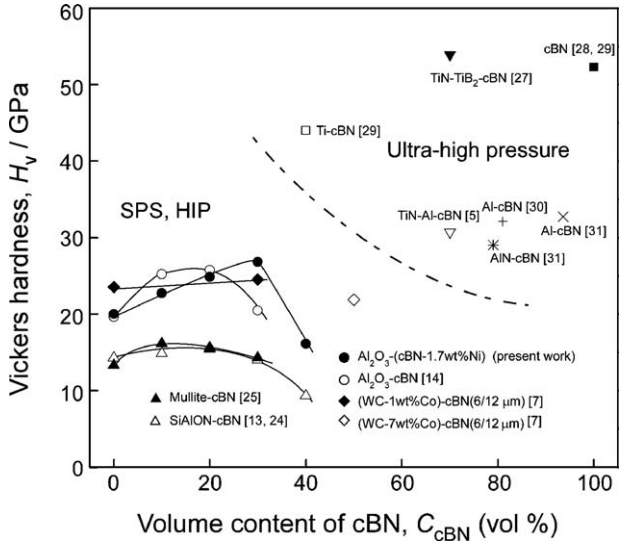

Fig. 8. Comparison of the highest hardness of cBN-containing composites between the present work and the reported values as a function of cBN volume content. The term "Ultra-high pressure" in this figure means several GPa.

mullite–cBN (16 GPa)[26] and WC–Co–cBN (25 GPa).[7,12] At $C_{cBN} > 40$ vol%, the cBN containing composites need an ultra-high pressure of over 5 GPa and at a high sintering temperature of over 1673 K. The highest reported H_v was 55 and 47 GPa of TiN–TiB_2–75 vol% cBN[27] and pure cBN[28,29] prepared at 5.5 GPa and 1720 K, and 7.7 GPa and 2473–2673 K, respectively. The H_v Al_2O_3–30 vol% (cBN/Ni) composite (27 GPa) is comparable to those high cBN content composites prepared at ultra-high pressure, i.e., Ti–40 vol% cBN ($H_v = 44$ GPa),[29] TiN–Al–75 vol% cBN ($H_v = 30.9$ GPa),[5] Al–93.6 vol% cBN ($H_v = 32.7$ GPa),[30] Al–81.4 vol% cBN ($H_v = 32.1$ GPa),[31] and AlN–78.9 vol% cBN ($H_v = 29$ GPa).[31]

4. Conclusions

Ni nanoparticles about 10–100 nm in diameter and 0.5–2.2 mass% in content were precipitated on cBN powder by RCVD. Al_2O_3–cBN/Ni composites were sintered by SPS at 1473–1673 K at a pressure of 100 MPa. The Al_2O_3–30 vol% cBN/Ni composite showed the highest values of $D_r = 99\%$ and $H_v = 27$ GPa at $C_{Ni} = 1.7$ mass% and $T_{SPS} = 1573$ K. The phase transformation of cBN to hBN was observed at the sintering temperature higher than 1573 K and at C_{Ni} higher than 1.7 mass%, and caused the decrease of D_r and H_v.

Acknowledgements

This research was financially supported by the Japan Society for the Promotion of Science (JSPS), Grant-in-Aids for JSPS fellow, 22-00365, JAPAN, the Rare Metal Substitute Materials Development Project, the New Energy and Industry Technology Development Organization (NEDO), the Global COE Program "Materials Integration (International Center of Education and Research), Tohoku University" and the International Collaboration Center, ICC-IMR, Tohoku University.

References

1. Wentorf RH, DeVries RC, Bundy FP. Sintered superhard materials. *Science* 1980;**208**:873–80.
2. Brookes K. Making hardmetal even harder with dispersed cBN. *Metal Powder Report* 2007;**62**(6):14–7.
3. Pierson HO. *Handbook of refractory carbides and nitrides*. William Andrew Publishing/Noyes; 1996.
4. Benko E, Klimczyk P, Mackiewicz S, Barr TL, Piskorska E. cBN-Ti_3SiC_2 composites. *Diamond and Related Materials* 2004;**13**(3):521–5.
5. Rong X-Z, Tsurumi T, Fukunaga O, Yano T. High-pressure sintering of cBN–TiN–Al composite for cutting tool application. *Diamond and Related Materials* 2002;**11**(2):280–6.
6. Benko E, Barr TL, Hardcastle S, Hoppe E, Bernasik A, Morgiel J. XPS study of the cBN–TiC system. *Ceramics International* 2001;**27**(6):637–43.
7. Martínez V, Echeberria J. Hot Isostatic Pressing of cubic boron nitride–tungsten carbide/cobalt (cBN–WC/Co) composites: effect of cBN particle size and some processing parameters on their microstructure and properties. *Journal of the American Ceramic Society* 2007;**90**(2): 415–24.
8. Omori M. Sintering, consolidation, reaction and crystal growth by the spark plasma system (SPS). *Materials Science and Engineering A* 2000;**287**(2):183–8.
9. Shen Z, Johnsson M, Zhao Z, Nygren M. Spark plasma sintering of alumina. *Journal of the American Ceramic Society* 2002;**85**(8):1921–7.
10. Nygren M, Shen Z. On the preparation of bio-, nano- and structural ceramics and composites by spark plasma sintering. *Solid State Sciences* 2003;**5**(1):125–31.
11. Zhang J, Wang L, Shi L, Jiang W, Chen L. Rapid fabrication of Ti_3SiC_2–SiC nanocomposite using the spark plasma sintering-reactive synthesis (SPS-RS) method. *Scripta Materialia* 2007;**56**(3):241–4.
12. Yaman B, Mandal H. Spark plasma sintering of Co–WC cubic boron nitride composites. *Materials Letters* 2009;**63**(12):1041–3.
13. Hotta M, Goto T. Densification and phase transformation of β-SiAlON–cubic boron nitride composites prepared by spark plasma sintering. *Journal of the American Ceramic Society* 2009;**92**(8):1684–90.
14. Hotta M, Goto T. Densification and microstructure of Al_2O_3–cBN composites prepared by spark plasma sintering. *Journal of the Ceramic Society of Japan* 2008;**116**(1354):744–8.
15. Lu J, Gao L, Gui L, Guo J. Preparation, thermal stability and sintering behavior of Ni/Al_2O_3 coated powders. *Materials Chemistry and Physics* 2001;**72**(3):352–5.
16. Li GJ, Huang XX, Guo JK. Fabrication and mechanical properties of Al_2O_3–Ni composite from two different powder mixtures. *Materials Science & Engineering A-Structural Materials Properties Microstructure and Processing* 2003;**352**(July (1–2)):23–8.
17. Moya JS, Rodriguez-Suarez T, Lopez-Esteban S, Pecharromán C, Torrecillas R, Díaz LA, et al. Diamond-like hardening of alumina/Ni nanocomposites. *Advanced Engineering Materials* 2007;**9**(10):898–901.
18. Tuan WH, Liu SM, Ho CJ, Lin CS, Yang TJ, Zhang DM. Preparation of Al_2O_3–ZrO_2–Ni nanocomposite by pulse electric current and pressureless sintering. *Journal of the European Ceramic Society* 2005;**25**(13):3125–33.
19. Zhang G, Jin Z, Yue X. TiN–TiB_2 composites prepared by reactive hot pressing and effects of Ni addition. *Journal of the American Ceramic Society* 1995;**78**(10):2831–3.
20. Kim H-C, Shon I-J, Yoon J-K, Doh J-M, Munir ZA. Rapid sintering of ultrafine WC–Ni cermets. *International Journal of Refractory Metals and Hard Materials* 2006;**24**(6):427–31.
21. JCPDS. International Centre for Diffraction Data, No. 10-173.
22. JPCDS. International Centre for Diffraction Data, No. 25-1033.
23. JPCDS. International Centre for Diffraction Data, No. 65-0380.
24. Benko E, Wyczesany A, Barr TL. CBN-metal/metal nitride composites. *Ceramics International* 2000;**26**(6):639–44.
25. Hotta M, Goto T. Spark plasma sintering of βSiAlON–cBN composite. *Materials Science Forum* 2007;**561/565**:599–602.
26. Hotta M, Goto T. Densification, phase transformation and hardness of mullite-cubic BN composites prepared by spark plasma sintering. *Journal of the Ceramic Society of Japan* 2010;**118**(1374):157–60.
27. Yoshida H, Kume S. Very high pressure sintering of cBN fine particles coated with TiN–TiB_2 layer formed by disproportionation reaction in molten salts. *Journal of Materials Research* 1997;**12**(3):585–8.
28. Taniguchi T, Akaishi M, Yamaoka S. Sintering of cubic boron nitride without additives at 7.7 GPa and above 2000 °C. *Journal of Materials Research* 1999;**14**(1):162–9.
29. Klimczyk P, Benko E, Lawniczak-Jablonska K, Piskorska E, Heinonen M, Ormaniec A, et al. Cubic boron nitride–Ti/TiN composites: hardness and phase equilibrium as function of temperature. *Journal of Alloys and Compounds* 2004;**382**(1–2):195–205.
30. Li YJ, Li SC, Lv R, Qin JQ, Zhang J, Wang JH, et al. Study of high-pressure sintering behavior of cBN composites starting with cBN–Al mixtures. *Journal of Materials Research* 2008;**23**(9):2366–72.
31. Lv R, Liu J, Li Y, Li S, Kou Z, He D. High pressure sintering of cubic boron nitride compacts with Al and AlN. *Diamond and Related Materials* 2008;**17**(12):2062–6.